Double Diffusive Convection by a Chebyshev Collocation Method

by

Alexandru Mihail MOREGA and Tatsuo NISHIMURA

(Received July 5, 1996)

Abstract

Solution accuracy is an important issue in modeling complicated, nonlinear physical phenomena such as double-diffusive processes. Recent researches in the area of internal, natural convection heat and mass transfer suggest that spectral methods may be a sound alternative to classical numerical schemes such as finite differences and finite element or, sometimes, the single one currently available.

The present work is aimed at assessing the ability of the spectral approach to solving strongly coupled double-diffusive convection processes previously analyzed by finite element methods. The good agreement with data reported in literature for the cases we investigated shows that Chebyshev collocation (pseudospectral) representation that was used results in a very accurate and reliable numerical scheme, with much potential in addressing transient regimes and nonlinear effects. When efficiently implemented, it leads to very performant, vectorized computer codes.

1. Introduction

Free convection due to spatial variations of fluid density is of fundamental importance in many natural and industrial problems [1]. Recently, increased interest was noticed regarding double-diffusive natural convection in chemical vapor transport processes and crystal-growth techniques of semiconductors and alloys, where temperature and concentration differences are evidently required [2], [3].

In a number of related numerical studies, diverse flow regimes have been investigated for different fluids. For example, Chang and Lin [4] examined thermosolutal convection in a salt-water solution at high Rayleigh numbers using a finite volume method. They found that the flow follows a quasi-periodic route to chaos under certain conditions. Shyy and Chen [5] analyzed the steady flow structures and stratification due to double-diffusive convection in liquids with low Prandtl number and demonstrated that with appropriate combinations of thermal Rayleigh and buoyancy ratio, multilayer structures appear in molten alloys. Nishimura et al. [6] studied the features of flow and associated heat and mass transfer for binary gases. Finite element solutions indicated that oscillatory flow occurs in a limited range of buoyancy ratios, which belongs to thermally-dominated convection.

However, most of numerical studies have paid less attention if any to the adequacy

Department of Mechanical Engineering, Yamaguchi University

of the numerical method employed to approach such problems. Recently, Ehrenstein and Peyret [7] and Hyun and Bergman [8] questioned whether conventional numerical methods (finite differences, finite element) are able or not to evidence the fine-scale phenomena typical to double-diffusive problems due to numerical difficulties for some ranges of Lewis number. On the other hand, spectral methods have been known for their high accuracy [9], [10]. Their advantage over classical methods is due mainly to the analytic nature of spectral approximation characterized by the fast decay in the approximation errors as spectral resolution is increased. However, this capability has not been proven enough yet, and motivates the present investigation.

We examined double-diffusion convection in a rectangular enclosure produced by opposite horizontal thermal and compositional buoyancy by a Chebyshev pseudospectral method and compared the results with previous solutions obtained by finite element method.

2. Problem Formulation

The working fluid confined in a rectangular cavity with no-slip, impermeable walls is assumed to be initially at rest. When temperature and concentration gradients are imposed, body forces are produced under gravitational field and convective motion may occur [11]. Provided that geometry and external constraints are such that all quantities are functions of (t,x,y) only (Fig. 1) the double diffusive convection process that occurs is completely described by a two-dimensional mathematical model consisting of:

vorticity (Navier - Stokes) and streamfunction equations for flow,

$$\frac{\partial \omega}{\partial t}+V\cdot\nabla\omega-Pr\Delta\omega=Pr\left(Ra_T\frac{\partial\theta}{\partial x}-Ra_S\frac{\partial c}{\partial x}\right), \tag{1}$$

$$\Delta\psi-\omega=0, \tag{2}$$

energy equation for heat transfer,

$$\frac{\partial\theta}{\partial t}+V\cdot\nabla\theta-\Delta\theta=0, \tag{3}$$

and species equation for mass transfer,

$$\frac{\partial c}{\partial t}+V\cdot\nabla c-\frac{1}{Le}\Delta c=0. \tag{4}$$

The following scaling is adopted,

$$\theta=\frac{T-T_C}{\Delta T},\ \Delta T=T_H-T_C,\ c=\frac{C-C_L}{\Delta C},\ \Delta C=C_H-C_L,$$

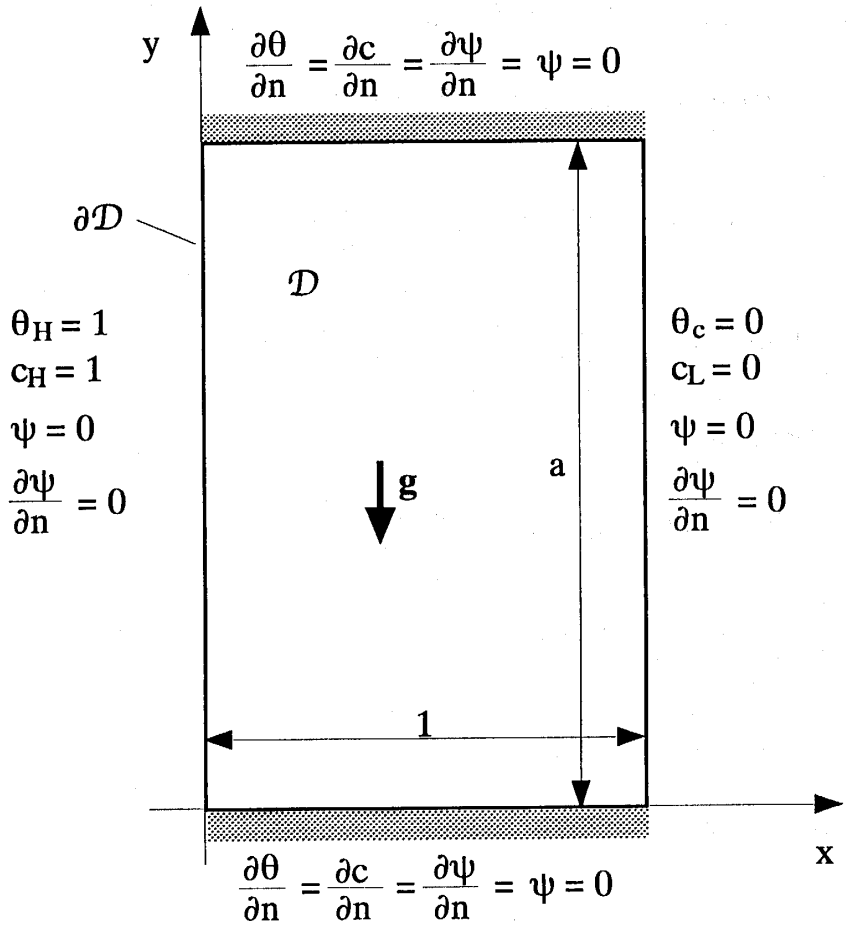

Figure 1 Computational domain, D and boundary conditions

$$(x,y) = \frac{(X,Y)}{L},\ a = \frac{H}{L},\ (u,v) = \frac{(U,V)}{\alpha/L},\ t = \frac{\tau}{L^2/\alpha},$$
$$Ra_T = \frac{g\beta_T \Delta T L^3}{\alpha\nu},\ Ra_S = \frac{g\beta_S \Delta C L^3}{\alpha D},\ Pr = \frac{\nu}{\alpha},\ Le = \frac{\alpha}{D}, \tag{5a}$$

where θ is the temperature, c is the species field, Ra_T, Ra_S are Rayleigh temperature and solute numbers, Pr is Prandtl number, Le is Lewis number, a is the cell aspect ratio (height/length), and velocity, $V = ui + vj$, vorticity, ω, and streamfunction, ψ, verify the following relations,

$$V = ui + vj = \frac{\partial\psi}{\partial y} i - \frac{\partial\psi}{\partial x} j,\ \omega = \frac{\partial v}{\partial x} - \frac{\partial u}{\partial y}. \tag{5b}$$

Streamfunction - vorticity formulation was preferred to eliminate the pressure from momentum equation and to reduce the number of unknowns [10]. Further more, the fluid is assumed to have constant properties and Boussinesq hypothesis is considered valid. Boundary conditions,

$$\psi(t,0,y)=\psi(t,1,y)=\psi(t,x,0)=\psi(t,x,a)=0, \tag{6a}$$

$$\frac{\partial\psi(t,0,y)}{\partial n}=\frac{\partial\psi(t,1,y)}{\partial n}=\frac{\partial\psi(t,x,0)}{\partial n}=\frac{\partial\psi(t,x,a)}{\partial n}=0, \tag{6b}$$

$$\theta(t,0,y)=1,\ \theta(t,1,y)=0,\ \frac{\partial\theta(t,x,0)}{\partial n}=0,\ \frac{\partial\theta(t,x,a)}{\partial n}=0, \tag{6c}$$

$$c(t,0,y)=1,\ c(t,1,y)=0,\ \frac{\partial c(t,x,0)}{\partial n}=0,\ \frac{\partial c(t,x,a)}{\partial n}=0, \tag{6d}$$

and initial conditions,

$$u(0,x,y)=\frac{\partial\psi(0,x,y)}{\partial y}=v(0,x,y)=-\frac{\partial\psi(0,x,y)}{\partial x}=0, \tag{7a}$$

$$\omega(0,x,y)=\frac{\partial v(0,x,y)}{\partial x}-\frac{\partial u(0,x,y)}{\partial y}0, \tag{7b}$$

$$\theta(0,x,y)=c(0,x,y)=0, \tag{7c}$$

close the mathematical model.

3. Numerical Method

A qualitative analysis of eqs. (1), (3) and (4) shows that-disregarding the r.h.s. of eq. (1) which may be seen as a source term-all quantities, ω, θ and c obey the same type of unsteady partial differential equation. Therefore, they may be solved by same method, detailed next for the case of streamfunction-vorticity (flow) problem (1)-(2). It is convenient to consider the r.h.s. of eq. (1) as a forcing term and note it, globally, through

$$f=Ra_T\frac{\partial\theta}{\partial x}-Ra_S\frac{\partial c}{\partial x}, \tag{8}$$

A three-level finite difference approximation in time, in which the diffusive term is treated implicitly and the convective term is evaluated explicitly, may be used to discretize eq. (1) leading to a family of semi-implicit schemes,

$$\frac{(1+\varepsilon)\omega^{n+1}-2\varepsilon\omega^{n}-(1-\varepsilon)\omega^{n-1}}{2\Delta t}+(2\theta_1+\theta_2)A^{n}+(1-2\theta_1-\theta_2)A^{n-1}-$$
$$Pr[\theta_1\Delta\omega^{n+1}+\theta_2\Delta\omega^{n}+(1-\theta_1-\theta_2)\Delta\omega^{n-1}]=f^{n+\alpha}, \tag{9}$$

and

$$\Delta\psi^{n+1}+\omega^{n+1}=0. \tag{10}$$

Here the upper index, $(\,)^n$, indicates the time step sequence, Δt is the time step and $A = \mathbf{V}\cdot\nabla\omega$ is the convective term. These schemes are shown [7], [9] to be at least first order accurate (in time), for an arbitrary choice of parameters ε, α, θ_1, θ_2, and second order accurate when

$$\varepsilon = 2(2\theta_1 + \theta_2 - 1) = 2\alpha. \tag{11}$$

We used $\varepsilon = 2$, $\theta_1 = 2$ and $\theta_2 = 0$, that is Adam-Bashforth second order backward Euler time marching scheme. In the case of Chebyshev approximation this scheme proves to be actually unconditionally stable. Equations (9) and (10) may be put in a compact form,

$$\begin{cases} \Delta\omega^{n+1} - \sigma\omega^{n+1} = F, \\ \Delta\psi^{n+1} + \omega^{n+1} = 0, \end{cases} \quad \text{in } D \tag{12}$$

with the boundary conditions,

$$\begin{cases} \psi^{n+1} = g^{n+1}, \\ \dfrac{\partial\psi^{n+1}}{\partial n} = h^{n+1}, \end{cases} \quad \text{on } \partial D \tag{13}$$

∂D is the boundary of the domain D and

$$\sigma = \frac{1+\varepsilon}{2\theta_1 Pr\Delta t} > 0, \tag{14}$$

is a constant coefficient in this two level constant time step method. At each time step a linear, Stokes-type domain problem, (12), with Dirichlet and Neumann boundary conditions, (13), has to be solved. As with all multi-level schemes, the first time step is treated differently: we assume that $\omega^{-1} = \omega^0$ and $A^{-1} = A^0$ so that the first solution is produced at $t = 2\Delta t/3$ and the actual solution at Δt is obtained by linear extrapolation.

When applying the finite difference time discretization discussed above to approximate temperature (3) and species (4) equations, the same type of problem as for vorticity [first eq. (12), Helmholtz type] are obtained. Therefore, the same numerical scheme for solving the resulting, approximate, domain problems may be used. We decided to solve Stokes problem (12)-(13) by Chebyshev collocation (pseudospectral) method, as introduced by Ehrenstein and Peyret [7]. In the class of spectral methods, the solution to the differential equation is seek in terms of a series of known, smooth functions. One basic reason for choosing Chebyshev rather than another representation (e.g. Fourier [12]) was motivated by the fact that the convergence properties of Chebyshev series are not affected by the boundary conditions but only by the smoothness of the unknown function (ω, ψ, θ, c) and its derivatives throughout the domain [9]. Consequently, Chebyshev expansion does not exhibit the Gibbs phenomenon at the boundaries, but at interior discontinuities of the function (ω, ψ, θ,

c), provided they occur. In the double diffusive problem under investigation the boundaries are likely to be more difficult to numerically approach rather than the interior of the cavity, therefore our choice for Chebyshev representation.

Chebyshev collocation solver for Stokes problem

By a coordinates transformation,

$$\xi = 2x - 1, \qquad \eta = \frac{2y - a}{a}, \tag{15}$$

the computational domain, D in fig. 1, $(x,y) \in [0,1] \times [0,a]$ can be mapped on the spectral computational domain, D, $(\xi,\psi) \in [-1,1] \times [-1,1]$, (fig. 2) usually used in the 2D Chebyshev collocation method. Here $\Gamma = \bigcup_{i=1}^{4} \Gamma_i$ is the boundary of D. Since the case when the cavity aspect ratio is not unity, $a \neq 1$, implies only trivial modifications in the coefficients that multiply η-derivatives, in what follows we assume that $a = 1$. Dropping the time step index, Stokes problem (12)-(13) may be written as,

$$\begin{cases} \Delta\omega - \sigma\omega = F, \\ \Delta\psi + \omega = 0, \end{cases} \qquad \text{in D} \tag{16}$$

$$\begin{cases} \psi = g, \\ \dfrac{\partial\psi}{\partial n} = h, \end{cases} \qquad \text{on } \Gamma \tag{17}$$

Continuity of g (18), compatibility of g and h (19) and compatibility of crossed

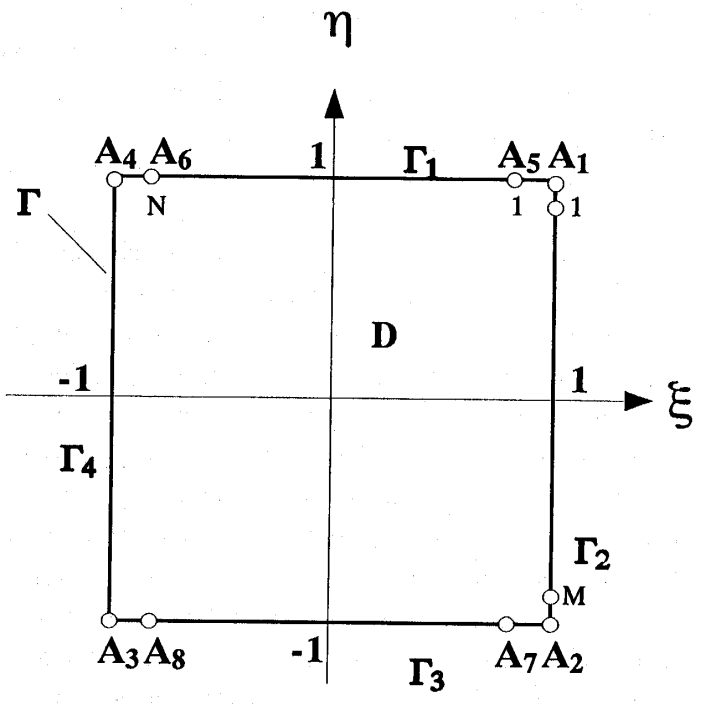

Figure 2 Spectral computational domain, D

derivatives of ψ (20) are imposed on the boundary conditions to ensure that y and its derivatives are defined on Γ, at the corners,

$$g_1(1)=g_2(1),\ g_2(-1)=g_3(1),\ g_3(-1)=g_4(-1),\ g_4(1)=g_1(-1), \tag{18}$$

$$\begin{aligned} &h_1(1)=g'_2(1),\ h_2(1)=g'_1(1),\ -h_3(1)=g'_2(-1),\ -h_4(1)=g'_1(-1),\\ &h_1(-1)=g'_4(1),\ h_2(-1)=g'_3(1),\ -h_3(-1)=g'_4(-1),\ -h_4(1)=g'_3(-1), \end{aligned} \tag{19}$$

$$h'_1(1)=h'_2(1),\ h'_1(-1)=-h'_4(1),\ h'_3(1)=-h'_2(-1),\ h'_3(-1)=h'_4(-1). \tag{20}$$

In Chebyshev representation, vorticity and streamfunction are written as products of polynomials,

$$(\omega_{N,M},\psi_{N,M})=\phi_N(\xi)\,\phi_M(\eta)=\sum_{n=0}^{N}\hat{\phi}_n T_n(\xi)\sum_{m=0}^{M}\hat{\phi}_m T_m(\eta), \tag{21}$$

where $\hat{\phi}_N$, $\hat{\phi}_M$ are constant coefficients (to be determined) and $T_n(\xi)$, $T_m(\eta)$ are Chebyshev polynomials of order n, m respectively. Usually, Chebyshev polynomial $T_n(\xi)$ is defined through,

$$T_n(\cos\theta)=\cos n\theta, \text{ when } \xi=\cos\theta. \tag{22}$$

In particular,

$$T_0(\xi)=1,\ T_1(\xi)=\xi,\ T_2(\xi)=2\xi^2-1,\ T_3(\xi)=4\xi^3-3\xi,\cdots \tag{23}$$

The collocation points (ξ_k,η_l), that constitute the discretization grid, defined through,

$$\begin{aligned} &\xi_k=\cos(k\pi/N), \qquad 0\leq k\leq N,\\ &\eta_l=\cos(l\pi/M), \qquad 0\leq l\leq M, \end{aligned} \tag{24}$$

are, typically, the abscissas of the $T_N(\xi)$, $T_M(\eta)$ respectively, extrema. By using recursion formulae [9], the derivatives that occur in Stokes problem may be expressed through,

$$\frac{d^p\phi_N(\xi_k)}{d\xi^p}=\sum_{j=0}^{N} d_N^{(p)}(k,j)\,\phi_N(\xi_j), \tag{25}$$

where p is the order of the derivative and $d_n^{(p)}$ are known, grid-dependent quantities [9]. Consequently, problem (16)-(17) assumes the following Chebyshev representation,

$$\begin{cases} \Delta\omega_{N,M}-\sigma\omega_{N,M}=F, \\ \Delta\psi_{N,M}+\omega_{N,M}=0, \end{cases} \qquad \text{in } D \tag{26}$$

$$\begin{cases} \psi_{N,M}=g, \\ \dfrac{\partial\psi_{N,M}}{\partial n}=h, \end{cases} \qquad \text{on } \Gamma. \tag{27}$$

When written at the collocation points (D_c, interior collocation points and Γ_c, boundary collocation points), eqs. (26) lead to an algebraic system of equations for the values of the polynomials $\omega_{N,M}$ and $\psi_{N,M}$ at the collocation points. It can be seen that the spectral problem (26)-(27) berries the same difficulty w.r.t. the boundary conditions as the original problem (16)-(17): two conditions for $\psi_{N,M}$ whereas none for $\omega_{N,M}$. Therefore, a method to produce a boundary condition for $\omega_{N,M}$ is needed. $\omega_{N,M}$ and $\psi_{N,M}$ are first decomposed [7] in,

$$\begin{aligned} \omega_{N,M} &= \tilde{\omega}_{N,M}+\bar{\omega}_{N,M}, \\ \psi_{N,M} &= \tilde{\psi}_{N,M}+\bar{\psi}_{N,M}. \end{aligned} \tag{28}$$

so that problem (26)-(27) may be split into two problems,

Problem $\mathbf{P}_1$,

$$\begin{cases} \Delta\tilde{\omega}_{N,M}-\sigma\tilde{\omega}_{N,M}=F, & \text{in } D_c \\ \tilde{\omega}_{N,M}=0, & \text{on } \Gamma_c \end{cases} \tag{29a}$$

$$\begin{cases} \Delta\tilde{\psi}_{N,M}+\tilde{\omega}_{N,M}=0, & \text{in } D_c \\ \tilde{\psi}_{N,M}=g, & \text{on } \Gamma_c, \end{cases} \tag{29b}$$

Problem $\mathbf{P}_2$,

$$\begin{cases} \Delta\bar{\omega}_{N,M}-\sigma\bar{\omega}_{N,M}=0, & \text{in } D_c \\ \Delta\bar{\psi}_{N,M}+\bar{\omega}_{N,M}=0, & \text{in } D_c \\ \begin{cases} \bar{\psi}_{N,M}=0, \\ \dfrac{\partial\bar{\psi}_{N,M}}{\partial n}=h-\dfrac{\partial\tilde{\psi}_{N,M}}{\partial n}=\bar{h}. \end{cases} & \text{on } \Gamma_c \end{cases} \tag{30}$$

Whereas $\mathbf{P}_1$ is a well formulated problem for both quantities, $\bar{\omega}_{N,M}$ and $\bar{\psi}_{N,M}$, the difficulty pointed out for problem (16)-(17) is now ported to $\mathbf{P}_2$: there are two boundary conditions for $\bar{\psi}_{N,M}$ but none for $\bar{\omega}_{N,M}$. Then $\mathbf{P}_2$ is reformulated, by prescribing Dirichlet boundary conditions, μ, for $\bar{\omega}_{N,M}$ such that Neumann condition for $\bar{\psi}_{N,M}$ is fulfilled,

Modified problem $\mathbf{P}_2$,

$$\begin{cases} \Delta\bar{\omega}_{N,M}-\sigma\bar{\omega}_{N,M}=0, & \text{in } D_c \\ \bar{\omega}_{N,M}=\mu, & \text{on } \Gamma_c \\ \Delta\bar{\psi}_{N,M}+\bar{\omega}_{N,M}=0, & \text{in } D_c \\ \bar{\psi}_{N,M}=0, & \text{on}\Gamma_c \\ \dfrac{\partial\bar{\psi}_{N,M}}{\partial n}=h-\dfrac{\partial\tilde{\psi}_{N,M}}{\partial n}=\bar{h}, & \text{on } \Gamma_c. \end{cases} \tag{31}$$

By boundary restrictions (19), the interpolating polynomial on the boundary, $\bar{h}_p$, that approximates Neumann boundary condition in (31) has to satisfy,

$$\bar{h}_{P_i}(\pm 1)=0, \qquad \bar{h}_{P_i}=\bar{h}_P|_{\Gamma_i}, \qquad 1\leq i\leq 4. \tag{32}$$

Four more conditions are implied by (20). Therefore, $\bar{h}_p$ is completely determined by its values at only $2(N+M-4)$ boundary collocation points $\Gamma'_c = \Gamma_c - \{A_1, A_2, ..., A_8\}$, where,

$$\begin{aligned} &A_1=(1,1), \quad A_2=(1,-1), \quad A_3=(-1,-1), \quad A_4=(-1,1), \\ &A_5=(x_1,1), \quad A_6=(x_{N-1},1), \quad A_7=(x_1,-1), \quad A_8=(x_{N-1},-1). \end{aligned} \tag{33}$$

On the other hand, Dirichlet boundary condition, m, needs to be prescribed at only $2(N+M-4)$ collocation points on the boundary (excluding the four corners and four extra, arbitrary points) to ensure the uniqueness of $\bar{\omega}_{N,M}$ in D_c [7]. By these two arguments, one can match the spectral spaces of the boundary conditions, μ and $\bar{h}_p$. It should be pointed out that by this method the spectral spaces of $\omega_{N,M}$ and $\psi_{N,M}$ have the same size and that $\bar{\omega}_{N,M}$ is uniquely defined only inside the domain. If the actual values of ω on the boundary are needed, one has to use ψ to compute them a posteriori, e.g. $\Delta\psi = -\omega$.

All is needed now is a procedure to obtain m form $\bar{h}_p$. Since the modified problem P_2 is linear, its solutions, $\bar{\omega}_{N,M}$ and $\bar{\psi}_{N,M}$, may be obtained by a superposition method: point-wise Dirichlet boundary conditions, $\rho_j(\eta_j) = 1$, $1 \leq j \leq J = 2(N+M-4)$, $\eta_j \in \Gamma'_c$, are assumed at the boundary collocation points on Γ'_c and J individual Stokes problems,

$$\begin{cases} \Delta\omega_j-\sigma\omega_j=0, & \text{in } D_c \\ \omega_j=\rho_j, & \text{on } \Gamma_c \\ \Delta\psi_j+\omega_j=0, & \text{in } D_c \\ \psi_j=0, & \text{on } \Gamma_c \end{cases} \tag{34}$$

are then solved. The seek boundary condition, m, and solutions $\bar{\omega}_{N,M}$, $\bar{\psi}_{N,M}$ are uniquely represented as linear combinations of these J unitary Dirichlet boundary conditions and solutions to (34), respectively

$$\begin{bmatrix} \mu \\ \bar{\omega}_{N,M} \\ \bar{\psi}_{N,M} \end{bmatrix} = \sum_{j=1}^{J} \lambda_j \begin{bmatrix} \rho_j \\ \omega_j \\ \psi_j \end{bmatrix}. \tag{35}$$

A compatible algebraic system of J equations is produced by applying Neumann condition [last eq. (31)] not yet used,

$$\mathbf{M}\Lambda=\bar{\mathbf{H}}, \tag{36}$$

where M is the "influence matrix" and,

$$\Lambda=[\lambda_1,\cdots,\lambda_J]^T,\ \bar{\mathbf{H}}=[\bar{h}_P(\eta_1),\cdots,\bar{h}_P(\eta_J)]^T,$$
$$\mathbf{M}=[m_{i,j}],\ m_{i,j}=\frac{\partial\psi_j}{\partial n}(\eta_i),\qquad 1\leq i,j\leq J. \tag{37}$$

Thus, the unknown influence coefficients, λ_j's may by determined from (36) by the direct method,

$$\Lambda=\mathbf{M}^{-1}\bar{\mathbf{H}}, \tag{38}$$

and further used to produce $\bar{\omega}_{N,M}$ and $\bar{\psi}_{N,M}$.

It is important to note that since all quantities in the J individual Stokes problems (34) are time-independent, the influence matrix, M, itself is time-independent, therefore it needs to be computed and inverted only once, at the beginning. However, the elements of vector $\bar{\mathbf{H}}$ are time-dependent and need to be computed at every time step.

Both problems $\mathbf{P}_1$ and modified $\mathbf{P}_2$ need a Helmholtz solver and, as it is used several times at every time step, this has to be very efficient. Therefore, a direct (one step) solver as suggested by [13], [14] and detailed next, was preferred.

Helmholtz solver

The general, non-homogeneous Helmholtz-Dirichlet problem may be written as,

$$\begin{cases}\Delta u-\sigma u=f, & \text{in D},\\ u=g, & \text{on }\Gamma.\end{cases} \tag{39}$$

When a spectral method is used to solve it, the following matrix equation is obtained,

$$\mathbf{D}_x^{(2)}\mathbf{U}_{N,M}+\mathbf{U}_{N,M}\mathbf{D}_y^{(2)T}-\sigma\mathbf{U}_{N,M}=F, \tag{40}$$

where, in the case of Chebyshev representation,

$$\mathbf{D}_x^{(2)}=[d_N^{(2)}(k,l)],\qquad 1\leq k,l\leq N-1, \tag{41a}$$

$$\mathbf{D}_y^{(2)}=[d_M^{(2)}(k,l)],\qquad 1\leq k,l\leq M-1, \tag{41b}$$

$$F=[F(\xi_k,\eta_l)],\qquad 1\leq k\leq N-1,\quad 1\leq l\leq M-1, \tag{41c}$$

$$F(\xi_k,\eta_l)=f(\xi_k,\eta_l)-d_M^{(2)}(l,0)g_1(\xi_k)-d_M^{(2)}(l,M)g_3(\xi_k)- d_M^{(2)}(k,0)g_2(\eta_l)-d_M^{(2)}(k,M)g_4((\eta_l). \tag{41d}$$

The eigenvalues of $\mathbf{D}_x^{(2)}$ and $\mathbf{D}_y^{(2)}$ ($\lambda_{x,1},...,\lambda_{x,N-1}$ and $\lambda_{y,1},...,\lambda_{y,M-1}$) are real, distinct and negative [14], therefore matrices (41a,b) are diagonalizable,

$$\begin{aligned}&\mathbf{S}_x^{-1}\mathbf{D}_x^{(2)}\mathbf{S}_x=\mathbf{diag}(\lambda_{x,1},\cdots,\lambda_{x,n-1})=\Lambda_x,\\&\mathbf{S}_y^{-1}\mathbf{D}_y^{(2)}\mathbf{S}_y=\mathbf{diag}(\lambda_{y,1},\cdots,\lambda_{y,M-1})=\Lambda_y.\end{aligned} \tag{42}$$

Here $\mathbf{S}_x$, $\mathbf{S}_y$ are the associated eigenvectors matrices. By pre-multiplying eq. (40) with $\mathbf{S}_x^{-1}$, to perform a first diagonalization (in x-direction), and post-multiplying it by $(\mathbf{S}_y^{-1})^T$, to perform a second diagonalization (in y-direction), a set of simple algebraic equations of the form,

$$(\lambda_{x,k}+\lambda_{y,k}-\sigma)\tilde{u}_{k,l}=\tilde{F}_{K,l},\qquad 1\leq k\leq N-1,\qquad 1\leq l\leq M-1, \tag{43}$$

that give $\tilde{u}_{k,l}$ is produced. Here $\tilde{u}_{k,l}$ are the entries of $\mathbf{S}_x^{-1}\mathbf{U}_{N,M}(\mathbf{S}_y^{-1})^T$ and $\tilde{\mathbf{F}}_{k,l}$ those of $\mathbf{S}_x^{-1}F(\mathbf{S}_y^{-1})^T$, respectively. From $u_{k,l}$ the solution $u_{N,M}(\xi_k,\eta_l)$ is further obtained.
It should be pointed out that other approaches are also possible. For example, the second diagonalization (in y-direction) may be replaced by directly solving the matrix equation obtained after x-diagonalization, possibly with preconditioning [15], to circumvent difficulties that might occur when $\mathbf{D}_y^{(2)}$ is ill-conditioned.
If Neumann rather than Dirichlet boundary condition is prescribed, representation formulae of type (25) may be used to project it on the solution spectral space.
Another important aspect is that matrices $\mathbf{D}_x^{(2)}$ and $\mathbf{D}_y^{(2)}$ are time-independent. Therefore, their eigen-spectra need to be solved only once, at the beginning.

Implementation

All elements needed to solve the unsteady double diffusive convection problem by Chebyshev collocation method are now available and may be put in the form of the following algorithm:

At the beginning:
construct the influence matrix, $\mathbf{M}$, and invert it;
compute the eigenvalues Λ_x, Λ_y and eigenvectors $\mathbf{S}_x$, $\mathbf{S}_y$ of $\mathbf{D}_x^{(2)}$ and $\mathbf{D}_y^{(2)}$;
At each time step:
solve problem $\mathbf{P}_1$ to obtain $\tilde{\omega}_{N,M}$ and $\tilde{\psi}_{N,M}$;
construct $\bar{\mathbf{H}}$;
construct Λ;
use the fast Helmholtz solver to calculate ($\omega_{N,M}$, $\psi_{N,M}$) as solutions of two (Helmholtz and Poisson) Dirichlet problems:

$$\begin{cases} \Delta\omega_{N,M} - \sigma\omega_{N,M} = F, & \text{in } D_c, \\ \omega_{N,M}(\eta_j) = \lambda_j, & \eta_j \in \Gamma'_c, \quad 1 \leq j \leq J, \\ \omega_{N,M} = 0, & \text{on } \Gamma_c - \Gamma'_c \end{cases}$$

$$\begin{cases} \Delta\psi_{N,M} + \omega_{N,M} = 0, & \text{in } D_c, \\ \psi_{N,M} = g, & \text{on } \Gamma_c. \end{cases}$$

use the fast Helmholtz solver to calculate $\theta_{N,M}$ as solutions of,

$$\begin{cases} \Delta\theta_{N,M} - \sigma_\theta\,\theta_{N,M} = F_\theta, & \text{in } D_c, \\ \theta_{N,M} = g_\theta, \text{ and/or } \dfrac{\partial\theta_{N,M}}{\partial n} = h_\theta & \text{on } \Gamma_c, \end{cases}$$

use the fast Helmholtz solver to calculate $c_{N,M}$ as solutions of,

$$\begin{cases} \Delta c_{N,M} - \sigma_c c_{N,M} = F_c, & \text{in } D_c, \\ c_{N,M} = g_c, \text{ and/or } \dfrac{\partial c_{N,M}}{\partial n} = h_c & \text{on } \Gamma_c. \end{cases}$$

The convective terms in F, $A = \mathbf{V}\cdot\nabla\omega$, F_θ, $\mathbf{V}\cdot\nabla\theta$ and F_c, $\mathbf{V}\cdot\nabla c$ are computed by matrix products in physical space using formulae of type (25) for derivatives.

A *Mathematica* [16] implementation of this algorithm was preferred in the development phase. Then, a double precision FORTRAN code implemented the algorithm. Specialized IMSL mathematical library routines [17] for matrix inversion, eigenvalues and eigenvectors (DEVCRG, DEPIRG, DLINRG) were used. We recall that these are needed only once, at the beginning. Our coding technique proved to be very efficient, ensuring a high vectorization level (>98%) [18] on the NEC SX-4 supercomputer of Yamaguchi University.

4. Results and Discussion

Previous numerical studies evidenced the existence of different double-diffusive flow regimes, according to the values of parameters in the governing equations, for instance steady or oscillatory solutions with possible hysteresis effects to initial conditions. However, the primary purpose of our research was to asses the modeling accuracy of Chebyshev pseudospectral method when applied to this category of flows rather than to investigate the physics of these phenomena.

In a first set of computations we considered the case when $a = 1$, $Pr = 1$, $Le = 2$, $Ra_T = 10^5$ and $Ra_S = 10^5$, that was studied by Nishimura et al. [19] through a finite element method. The fluid confined in a square enclosure is initially stagnant, with neither temperature nor concentration gradients, and the vertical walls are kept at the same uniform temperature, $\theta = 0$, and concentration, $c = 0$. At time $t = 0$ the left wall exhibits a abrupt change in temperature and concentration conditions, that are suddenly raised at a higher level, $\theta = 1$ and $c = 1$. We modeled the transient regime towards the final steady state, eventually reached by the system and shown in Fig. 3 through streamfunction, temperature and concentration contours. Although the flow is

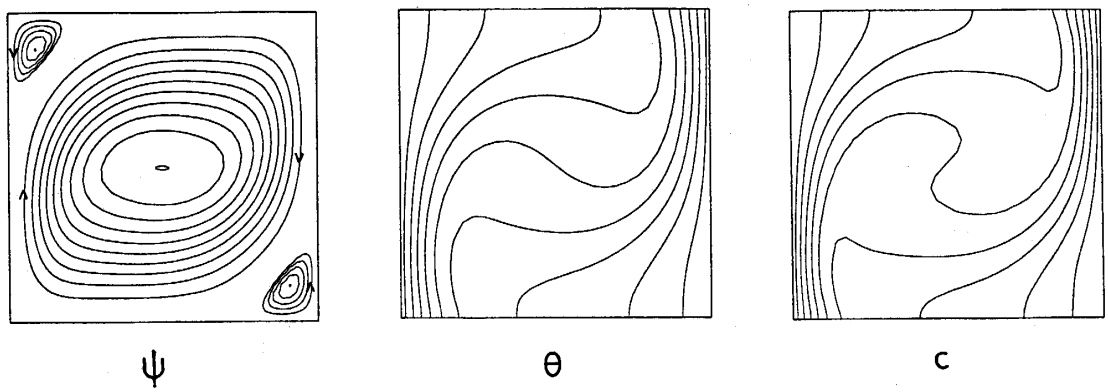

Figure 3 Steady state streamlines, temperature and concentration contours for $a = 1$, $Pr = 1$, $Le = 2$, $Ra_T = Ra_S = 10^5$

Table 1. Comparison between the two numerical methods for $a = 1$, $Pr = 1$, $Le = 2$, $Ra_T = Ra_S = 10^5$

	Pseudospectral method (40 × 40 points)	Finite element method (26 × 26 points)
ψ_{min}	-10.68	-10.45
ψ_{max}	0.102	0.13
Nu	3.01	3.09
Sh	3.82	3.85

dominated by thermal buoyancy forces, as indicated by the large central clockwise rotating vortex in the core of the enclosure, the effects of compositional forces are observed through two counter-clockwise rotating vortices at the high- and low -concentration walls, in the upper and lower corners, respectively. Temperature and concentration contour lines agree well with those obtained by the finite element method, though not shown here. Table 1 compares some relevant results as produced by the two numerical schemes: streamfunction extrema, ψ_{min} and ψ_{max}, which indicate the strength of thermal and compositional vortices; average Nusselt, Nu, and Sherwood, Sh, numbers along the hot wall. A small discrepancy may be noted for ψ_{max}, but the agreement is satisfactory for all other physical quantities. This may be explained by the shift of ψ_{max} actual location w.r.t. the collocation mesh: while ψ_{min} occurs in the cavity center, where a mesh node exists, ψ_{max} is not necessarily found at collocation points where results are reported.

We considered next the case of an oscillatory flow when $a = 2$, $Pr = 1$, $Le = 2$, $Ra_T = 10^5$ and $Ra_S = 10^5$ studied by Nishimura et al. [6] with same initial and boundary conditions as in the first case. Figure 4 shows the time variation of ψ_{min} and ψ_{max} , indicating a periodic oscillatory flow with a period 0.0494. The thermal vortex strength is about five times larger than the compositional one and there is a 90 ° phase shift between them. Figure 5 displays streamfunction, temperature and concentration contours at four moments during a period of oscillation, marked in Fig. 4. At time

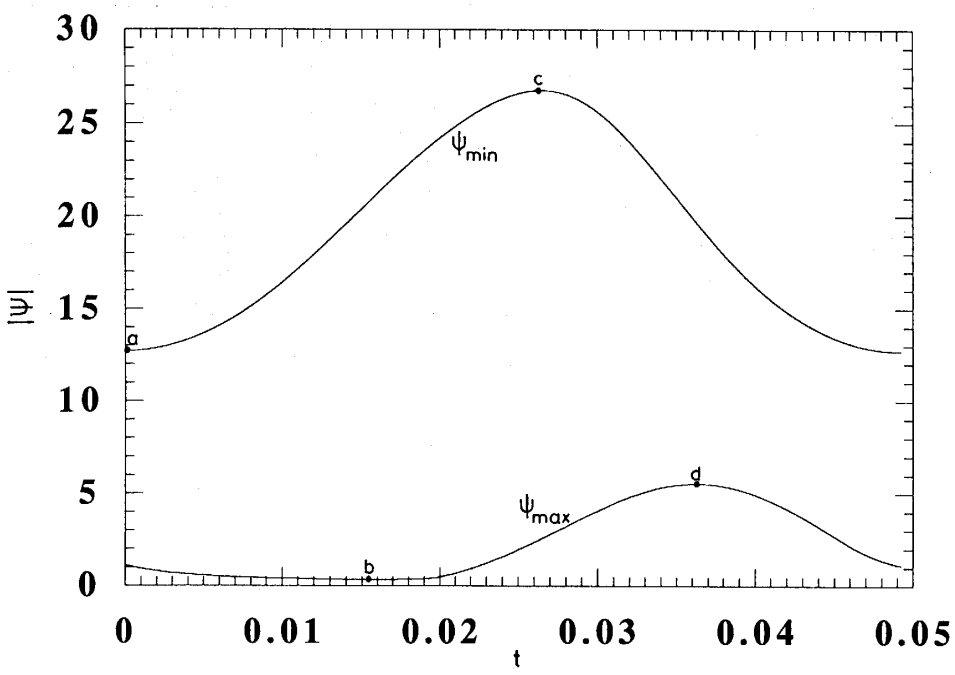

Figure 4 Streamfunction extrema for a period of oscillation in the case a = 2, Pr = 1, Le = 2, $Ra_T = Ra_S = 10^5$

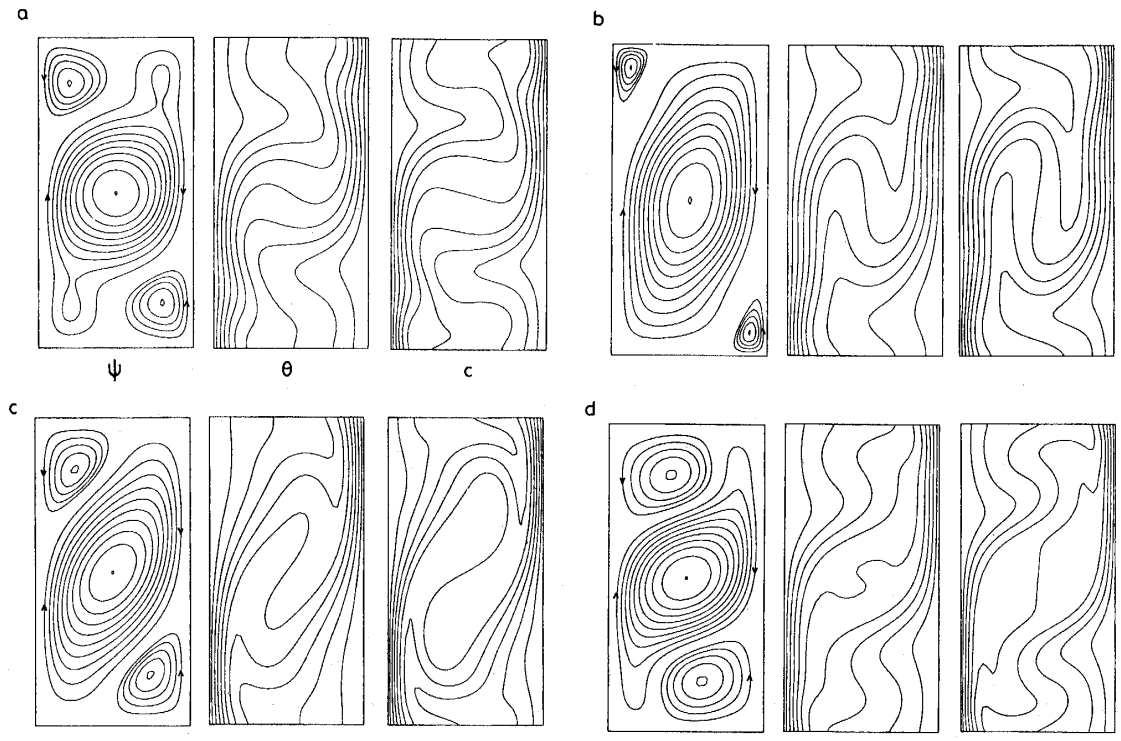

Figure 5 Streamlines, temperature and concentration contours for a = 2, Pr = 1, Le = 2, $Ra_T = Ra_S = 10^5$

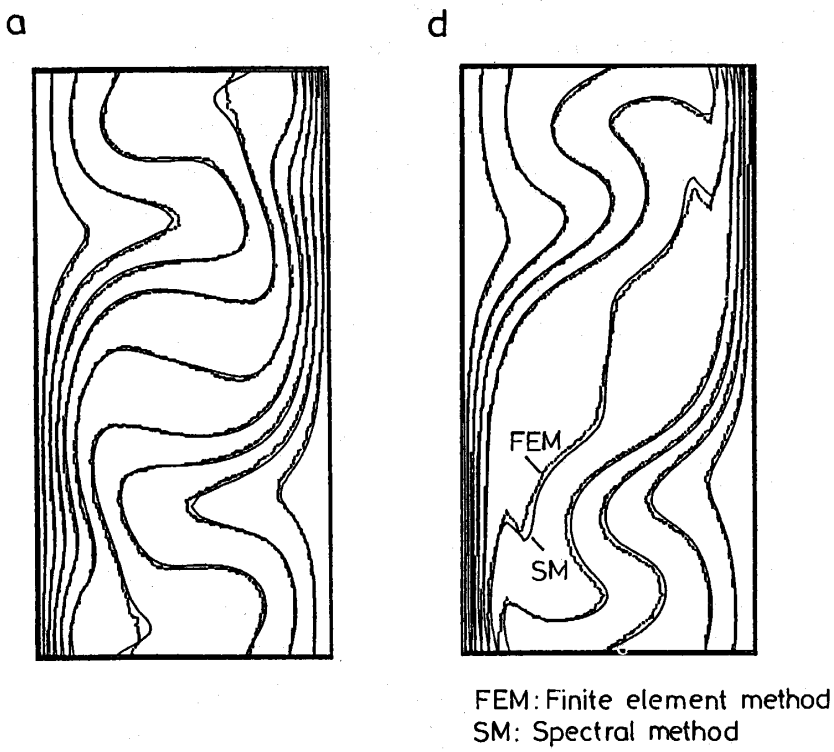

Figure 6 Temperature and concentration contours: a comparison between FEM and SM results for a = 2, Pr = 1, Le = 2, $Ra_T = Ra_S = 10^5$

Table 2. Comparison between the two numerical methods for a = 2, Pr = 1, Le = 2, $Ra_T = Ra_S = 10^5$

	Pseudospectral method (40 × 80 points)	Finite element method (31 × 41 points)
Period	0.0494	0.0497
Max ψ_{min}	-26.8	-26.7
Min ψ_{min}	-12.7	-12.9
Max ψ_{max}	5.52	5.76
Min ψ_{max}	0.333	0.351

moment (a) the thermal vortex reaches its minimum. Two regions of unstable and stable stratification of concentration are located at the central part and in the upper and lower regions of the enclosure, respectively. At time moment (b) the compositional vortex attains its minimum. The unstable stratification zone in the core tends to diminish with the growth of the thermal vortex. At time moment (c) the thermal vortex is at its maximum and the region of stable stratification dominates the core, contrasting with case (a). At time moment (d), when the compositional vortex reaches its maximum, the stable stratification in the central part is seen to diminish with the thermal vortex decrease. Thus, the global oscillatory flow evidences a periodic

exchange between stable and unstable states in species stratification, due to interactions between thermal and compositional vortices.

In Fig. 6 pseudospectral and finite element results are compared in terms of concentration contours at time moments (a) and (d) (fine line for pseudospectral solution and a notched line for finite element output). The good agreement confirms the numerical accuracy of both methods. Some physical quantities computed by the two methods and listed in Table 2 show that the finite element method (for 31×41 nodal points) provides accurate results.

Finally, we consider the transient double-diffusive process studied by Kamakura

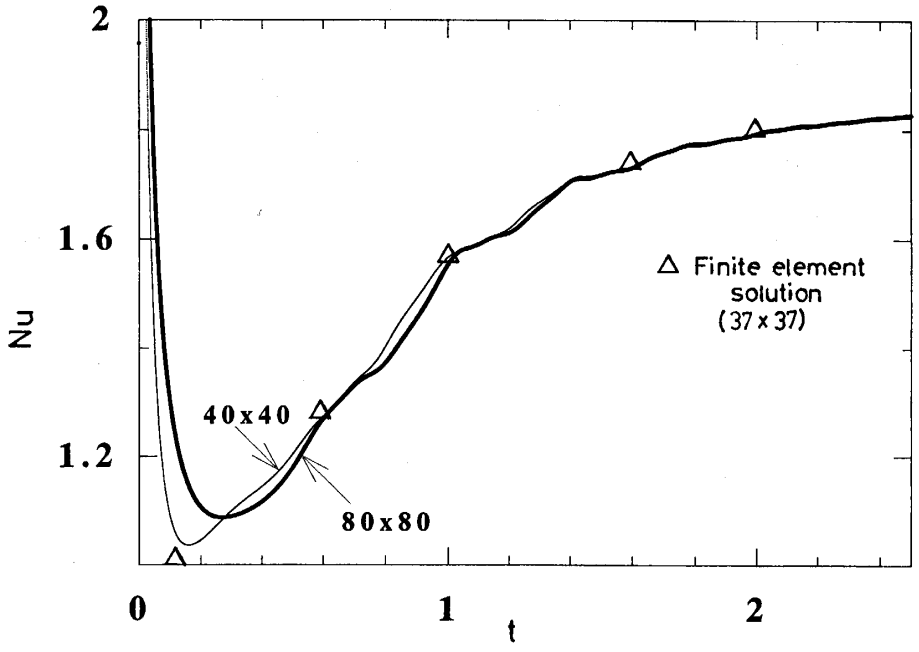

Figure 7 Average Nu number time evolution in the case a = 1, Pr = 0.01, Le = 100, $Ra_T = 10^5$, $Ra_S = 2\times10^4$

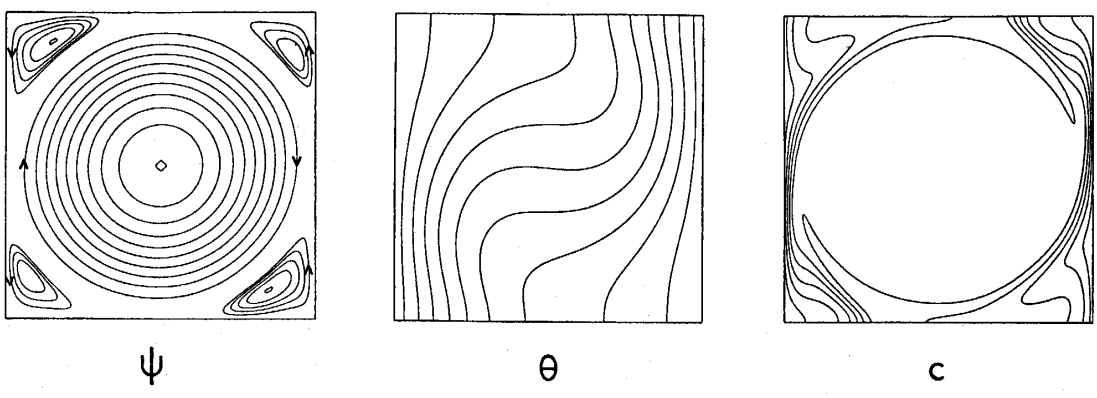

Figure 8 Steady state streamlines, temperature and concentration contours for a = 1, Pr = 0.01, Le = 100, $Ra_T = 10^5$, $Ra_S = 2\times10^4$

and Ozoe [20], with a = 1, Pr = 0.01, Le = 100, $Ra_T = 10^4$, $Ra_S = 2\times10^4$. Figure 7 shows the dynamics of the process through the average Nusselt number. It is notable that a fine meshing is needed to precisely represent the early stage and that finite element solution (37×37 nodal points) is especially accurate in the late stage, towards steady state. Figure 8 displays the steady state solutions. The flow in the cavity is dominated by a thermal vortex and the concentration field in the core is seen more uniform than temperature, which are typical for a high Lewis number double-diffusive regime.

From the above results for steady and periodic, time-dependent double-diffusive problems which were investigated, we conclude that in terms of accuracy Chebyshev pseudospectral method is comparable with finite element method for steady states, but superior for transient regimes and strong nonlinear effects.

5. Conclusions

This work was aimed at assessing the ability of Chebyshev pseudospectral method to accurately represent the dynamics of complicated, strongly coupled convective processes such as natural double-diffusive heat and mass transfer. Steady and unsteady flow regimes previously analyzed through finite element methods were solved by this technique and the results obtained are in good agreement with archived ones, indicating that this method is a reliable modeling tool.

It contrasts with classical methods through its analytic origins: the solution is seek in the spectral space, in terms of known, smooth functions, rather than low order basis or grid functions.

In our experience, transient regimes and strong nonlinear effects are better addressed through spectral techniques and, for same mesh sizes, they should produce more accurate results than classical methods. Most notably, it is particularly efficient in modeling boundary layer effects when Chebyshev polynomials representation is used.

Their apparent limited application to simple geometries may be relieved through mesh generation techniques commonly used with classical methods such as finite differences. The two level, constant time step scheme we used is only one option, other time marching schemes being possible as well.

An important feature is that the numerics involved by Chebyshev collocation (pseudospectral) method reduces to matrix operations which, through efficient programming techniques, may be implemented into very performant codes, especially on vector machines.

References

1. Chen, C. F. and Johnson, D. H., "Double diffusive convection: a report on an engineering foundation conference," *J. Fluid Mech.*, **138**, p.405, 1984.
2. Ostrach, S., "Fluid dynamics in crystal growth - the 1982 Freeman Scholar Lecture", *ASME J. Fluid Eng.* **105**, pp.5-20, 1982.
3. Berkermann, C. and Viskanta, R., "Mathematical modeling of transport phenomena during alloy

solidification," *Appl. Mech. Rev.*, **46**, pp.1-27, 1993.
4. Chang, J. and Lin, T. F., "Unsteady thermosolutal opposing convection of liquid-mixture in a square cavity-II flow structure and fluctuation analysis," *Int. J. Heat Mass Transfer,* **36**, pp.1333-1345, 1993.
5. Shyy, W. and Chen, M-H., "Double-diffusive flow in enclosures," *Phys. Fluids A,* **3**, pp.2592-2607, 1991.
6. Nishimura, T., Wakamatsu, M. and Kunitsugu, K., "Oscillatory double-diffusive convection in a rectangular enclosure with combined horizontal temperature and concentration gradients," Numerical Methods in Thermal Problems, **9**, pp.100-111, 1995.
7. Ehrenstein, U. and Peyret, R., "A Chebyshev collocation method for the Navier-Stokes equations with applications to double-diffusive convection," *Int. J. Numer. Methods Fluids,* **9**, pp.427-452, 1989.
8. Hyun, M. T. and Bergman, T. L., "Direct simulation of double-diffusive layered convection," *ASME J. Heat Transfer,* **117**, pp.334-339, 1995.
9. Gottlieb, D. and Orszag, S. A., *Numerical analysis of spectral methods: theory and applications,* SIAM (1977), Regional Conf. Series in Appl. Math.
10. Peyret, R. and Taylor, T. D, *Computational methods for fluid flow,* Springer Series in Computational Physics, Springer Verlag NY, 1990.
11. Bejan, A., *Convection heat transfer,* Wiley, NY, 1984.
12. Kimura, S., Schubert, G. and Straus, J. M., "Route to chaos in porous-medium thermal convection," *J. Fluid Mech.*, **166**, pp.305-324, 1986.
13. Haldenwang, P., Labrosse, G. and Abboudi, S., "Chebyshev 3-D spectral and 2-D pseudospectral solvers for the Helmholtz equation," *J. Comput. Phys.*, **55**, pp.115-128, 1984.
14. Gottlieb, D. and Lustman, L., "The spectrum of the Chebyshev collocation operator for the heat equation," *SIAM J. Numer. Anal.,* vol. **20**, no.5, pp.909-921, 1983.
15. Canuto, C. and Quateroni, A., "Preconditioned minimal residual methods for Chebyshev spectral calculations," *J. Comput. Phys.*, **60**, pp.315-337, 1984.
16. Wolfram, St., *Mathematica. A system of doing mathematics by computer,* v.2.2, 1993.
17. IMSL Math/Library. FORTRAN subroutines for mathematical applications. Visual Numerics, Inc., 1994.
18. *News Letter of Yamaguchi Computing Center,* **254**, June 11, 1996.
19. Nishimura, T., Imoto, T. and Wakamatsu, M., "A numerical study of the structure of double-diffusive natural convection in a square cavity," ASME/JSME Thermal Engineering Conference, vol. 1, pp.193-200, ASME 1995.
20. Kamakura, K. and Ozoe, H., "Oscillatory double diffusive natural convection in low Pr fluid," 33rd Conference on Heat Transfer, Niigata, Japan, 1996.